Modelling, Simulation and Experimental Validation of Half Semi-Truck Suspension System Vibration

H. K. Ibrahim[1]*, O. T. Popoola[1], E. A. Akinola[2], F. W. Osatuyi[3], Z. O. Tijani[4], K. O, Abdulazeez[4], F. O. Mustapha[5], T. M. Kelani[1]

[1]Department of Mechanical Engineering, University of Ilorin, Nigeria
[2] Department of Mechanical and Material Engineering, University of Nebraska-Lincoln, USA
[3]Mechanical Engineering Unit, Krone, Nigeria
[4]Maintenance Department, Dangote Refinery and Petrochemicals FZE, Nigeria
[5]Product Business Management Division, GIL Automations, Lagos, Nigeria

ABSTRACT: This paper is aimed at modelling and experimental validation of the vibration models of a semi-truck suspension system. A half-car (4-degree-of-freedom) model was developed for the semi-truck vehicle using the Newton law and simulated using SCILAB-Xcos. The analysis specifically focused on the acceleration response of the vehicle body at different speed levels (10, 20, and 30 km/hr), which was determined with the smartphone-installed accelerometer (Keuwl app). The simulated root mean square accelerations of 0.33, 0.55 and 0.72 m/s^2 revealed a favourable comparison with the experimental root mean square accelerations (0.31, 0.54 and 0.69 m/s^2) at 10, 20 and 30 km/hr, respectively. This showed that the ride comfort is not an uncomfortable zone at low speeds, and many are considered fairly uncomfortable. The findings provided valuable insights into the dynamic behaviour of semi-truck vehicles, highlighting the role of speed in suspension system performance. This information can be utilised to optimise vehicle performance, enhance ride comfort, and improve overall safety.

KEYWORDS: Modelling, Simulation, Ride comfort, Half-car model, and Vibration

[Received Nov. 11, 2024; Revised Jan 31, 2025; Accepted Feb. 14, 2025] Print ISSN: 0189-9546 | Online ISSN: 2437-2110

I. INTRODUCTION

The suspension system is integral to the vehicle to achieve vehicle safety and comfort (Nguyen, 2021). It is a mechanism that physically isolates the car body from the wheels, thereby preventing the road excitations experienced by the tires to the users (Atindana *et al.,* 2023). The excitations could be caused by unbalanced wheels, potholes, unfilled trenches, bridge gaps, road bumps and humps, and uneven and ungraded roads, which affect the comfort of the users, especially in developing economies (Ojolo *et al.,* 2021). As a result, the excitation measurement is crucial in providing quality information on road damage prediction, accident handling, building structure monitoring, and machine and vehicle shock (suspension system) vibration analyses.

Conventional vibration analyses and measuring devices available today are generally expensive, complicated, and not always easily accessible to everyone (Riley, 2023). An accelerometer is a feasible and efficient road-monitoring device that provides vibrating signals (Casati *et al.,* 2020). Accelerometers are generally capable of measuring the force accompanying motion, and according to Newton's second law of mechanics, force is proportional to acceleration (Ibrahim *et al.,* 2020). It has been reported that ADXL345 accelerometers were used as part of a vibration-based system to monitor the structural health of bridges, ATmega16 microcontroller-based accelerometers, and a PC display are used to measure and monitor the vibration level of an object or system and NodeMCU ESP 32 and smartphone as a data display (Hapsari *et al.,* 2021).

The smartphones are also equipped with sophisticated sensing capabilities that allow the installation of numerous applications (*apps*) and assist in environmental sensing and infrastructure monitoring (Ibrahim *et al.,* 2020). Rana and Asaduzzaman (2021) utilised a smart device accelerometer to estimate the acceleration, orientation, shock, vibration, velocity, speed, and position of vehicles. Casati *et al.* (2020) utilised smartphone accelerometer data to detect the vibration impact of vehicles in a speed bump using a smartphone with the KaptAccel app. Other smartphone accelerometer apps for vibration analyses include the PhyPhox app (Riley, 2023), the iDynamics app (Feldbusch *et al.,* 2017), and the Keuwl accelerometer app, all accessible on iOS and Android. The results from the Apps displayed the acceleration and velocity information and their respective maximum values obtained during the measurement and processing of vibrating systems (Ginart *et al.,* 2011).

Experimental data from vibration measurements have been validated to provide robust models for vibration raw data processing and classification with indispensable tools, offering valuable insights into the dynamic behaviour and performance of the systems (De La Torre *et al.,* 2020; Jia and Sharma, 2021). Dynamic system modelling and simulation have become required in the system design process to describe and predict the interactions over time between multiple components of complicated systems without conducting

*Corresponding author: ibrahim.kh@unilorin.edu.ng
doi: http://dx.doi.org/10.4314/njtd.v22i1.3076

expensive and time-consuming experiments (Yaabari *et al.,* 2023). Some complex methods utilised for vibration analyses of vehicle suspension systems to improve ride comfort and road handling such as interval type-2 fuzzy control (Yatak and Şahin, 2021), ARX model-based predictive control (Piñón *et al.,* 2021) and PID-SMC synthetic control algorithm (Nguyen, 2023). MATLAB- Simulink has been utilised for vibration model simulations and experimental validation of vibration system analyses (Khemliche *et al.,* 2004). For example, Tiwari and Bhavikatti (2020); Phalke and Mitra (2017); Puneet *et al.* (2019) and Bhagyasri and Chaitanya (2019) utilised MATLAB-Simulink to solve the equation of vehicle suspension models to study vibration analyses and find out the effect stiffness, damping coefficient, sprung mass and velocity on ride comfort and road holding. The results obtained with the vehicle-human interaction were well within ISO 2631-1-1997 standard.

Recently, using SCILAB software, Bovnegra and Strelbitskyi (2022) developed a mathematical model to investigate a mass-spring-damper system's dynamic behaviour. The results are similar to the results obtained from MATLAB, which suggests Scilab is good enough for simulations as an alternative to paid software like MATLAB. SCILAB-xCos is like MATLAB-Simulink module utilised by researchers and engineers to study the vehicle suspension systems behaviours, leading to better suspension designs, more comfortable rides, and greater vehicle performance. In this study, the vibration analysis of a half-truck suspension was modelled, simulated using SciLab-Xcos, and experimentally validated.

.

II. METHODOLOGY

A. Semi-Truck Suspension Model

The half model of a semi-truck with a two-wheel drive was mathematically developed, shown in Figure 1, with one front and one back wheel. The excitations due to the road surface were applied as specified displacement at the wheel's point of contact with the road. Application of the condition of equilibrium results in a set of linear second-order differential equations of motion in Equation 1 as follows:

$$M\ddot{X} + C\dot{X} + KX = \sum F(t) \quad (1)$$

where M, C and K represent the system's mass, damping and stiffness matrices, respectively, and F(t) represents the excitation force vector. The Centre of Gravity (CoG) is located as shown in Figure 1. L_1 and L_2 are the distances from the CoG to the shock absorbers. Other parameters include the stiffness (K_{fs}) and damping coefficient (C_{fs}) of the Front Shock Absorbers while the stiffness (K_{rs}) and damping coefficient (C_{rs}) are parameters for the Rear Shock Absorbers. The equation of motion of the vehicle model was derived with a rigid body shown in Figure 2, with the sprung mass, suspension axle mass and unsprung mass represented as M_1, M_2 and M_3, respectively.

For the half semi-truck model, the road unevenness input into the system at both the front and rear tires was represented with X_R and X_G in Figure 2.

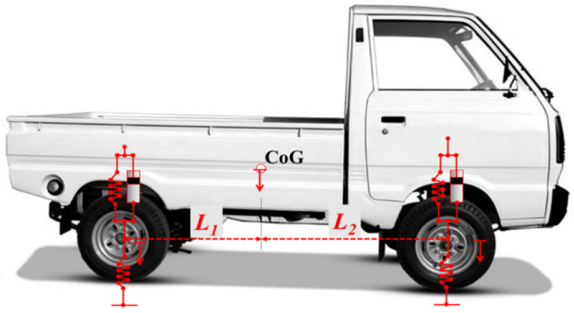

Figure 1: A Semi-Truck Vehicle showing the suspension details

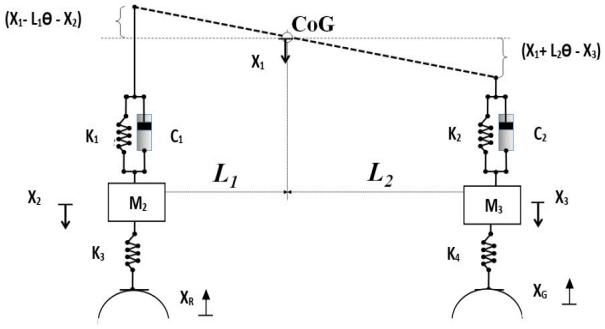

Figure 2: Free Body Diagram of the Model

The input of road elevation to the front and rear tires were separated by a time delay function in Eq. 2 and 3 as follows:

$$X_R(t) = X_G(t - \tau) \quad (2)$$

This time delay, τ, is a function of the distance between the front and rear tires and the vehicle's forward-moving velocity:

$$\tau = \frac{(L_1 + L_2)}{v} \quad (3)$$

1. System Equation of Motion

The equation of motion derived from the semi-truck suspension model is given in equations 4 to 7 as follows:

$$M_1\ddot{X}_1 = -(K_1 + K_2)X_1 + K_1X_2 + K_2X_3 + (K_1L_1 - K_2L_2)\theta - (C_1 + C_2)\dot{X}_1 + C_1\dot{X}_2 + C_2\dot{X}_3 + (C_1L_1 - C_2L_2)\dot{\theta} \quad (4)$$

$$M_2\ddot{X}_2 = K_1X_1 - (K_1 + K_3)X_2 - K_1L_1\theta - K_3X_R - C_1\dot{X}_2 + C_1\dot{X}_1 - C_1L_1\dot{\theta} \quad (5)$$

$$M_3\ddot{X}_3 = K_2X_1 - (K_2 + K_4)X_3 + K_2L_2\theta + K_4X_G - C_2\dot{X}_3 + C_2\dot{X}_1 + C_2L_2\dot{\theta} \quad (6)$$

$$J\ddot{\Theta} = (K_1L_1 - K_2L_2)X_1 - K_1X_2L_1 + K_2X_3L_2 - (K_1{L_1}^2 + K_2{L_2}^2)\theta + (C_1L_1 - C_2L_2)\dot{X}_1 - C_1\dot{X}_2L_1 + C_2\dot{X}_3L_2 - (C_1{L_1}^2 + C_2{L_2}^2)\dot{\theta} \quad (7)$$

The equations above were transformed into the matrix in Eq. 8.

$$\begin{bmatrix} M_1 & 0 & 0 & 0 \\ 0 & M_2 & 0 & 0 \\ 0 & 0 & M_3 & 0 \\ 0 & 0 & 0 & J \end{bmatrix} \begin{Bmatrix} \ddot{X}_1 \\ \ddot{X}_2 \\ \ddot{X}_3 \\ \ddot{\Theta} \end{Bmatrix} + \begin{bmatrix} C_1 + C_2 & -C_1 & -C_2(C_2L_2 - C_1L_1) \\ -C_1C_1 & 0 & C_1L_1 \\ -C_2 & 0 & C_2 \\ (C_2L_2 - C_1L_1)C_1L_1 & & -C_2L_2 \\ & & -C_2L_2(C_1{L_1}^2 - C_2{L_2}^2) \end{bmatrix} \begin{Bmatrix} \dot{X}_1 \\ \dot{X}_2 \\ \dot{X}_3 \\ \dot{\theta} \end{Bmatrix} + \begin{bmatrix} K_1 + K_2 & -K_1 & -K_2(K_2L_2 - K_1L_1) \\ -K_1K_1 & 0 & K_1L_1 \\ -K_2 & 0 & K_2 \\ (K_2L_2 - K_1L_1)K_1L_1 & & -K_2L_2 \\ & & -K_2L_2(K_1{L_1}^2 - K_2{L_2}^2) \end{bmatrix} \begin{Bmatrix} X_1 \\ X_2 \\ X_3 \\ \theta \end{Bmatrix} = \begin{Bmatrix} 0 \\ -K_3X_R \\ -K_4X_G \\ 0 \end{Bmatrix} \quad (8)$$

The force vector for this system is represented by F(t) and is given in equation 9 as follows:

$$F(t) = [0 \quad -K_3X_R(t) \quad -K_4X_G(t) \quad 0]^T \quad (9)$$

The speed vector X(t) of the system is given in Eq. 10 as follows:

$$X = [X_1(t)X_2(t)X_3(t) \quad \theta(t)]^T \quad (10)$$

B. Vibration Experiments of Semi-Truck Suspension System

In order to validate the theoretical model, a JMC Pickup truck with chassis JX1020TSD5 shown in Figure 3 has a four-wheel drive and an Android phone installed with a mobile accelerometer app with the interface with responses along X, Y and Z axes shown in Figure 4. The experiment was carried out at Pipeline Road along, Tanke Ilorin at a latitude of 8.47269° N and a longitude of 4.5928° E, Kwara State, Nigeria, with many 0.08 m Bumps shown in Figure 5. The accelerometer was placed at the front seat of the half model of the semi-truck in the direction shown in Figure 6 and the detailed direction shown in Table 1 to achieve a vertical excitation effect (X-direction) while in motion at different fixed speeds (10, 20 and 30 km/h) over the undulation without applying brakes. The data were saved on the accelerometer for validation and analysis. The bump profile used was 8.80 m in width, 0.85 m in length and 0.15 m height. The SCILAB software was used to analyse the response of the vehicle. The experimental data was collected using a smartphone at the centroid position of a Semi-Truck Vehicle.

Figure 3: The JMC Pickup truck at the site of the experiment

Figure 4: The Mobile Accelerometer Interface used for the Experiment

The same experiment above was carried out with brakes/slowing down over the road undulation (bump) of 0.05 and 0.08m height at the same speeds as above, and the data were also logged.

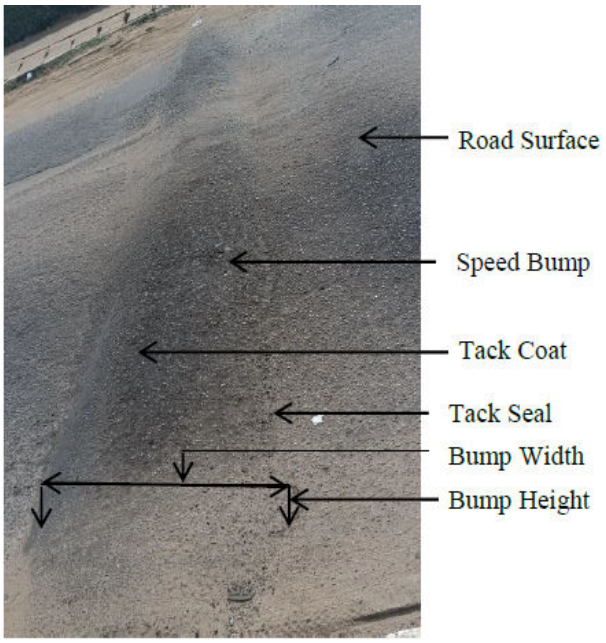

Figure 5: Single Road Undulation (Bump) used for the Experiment

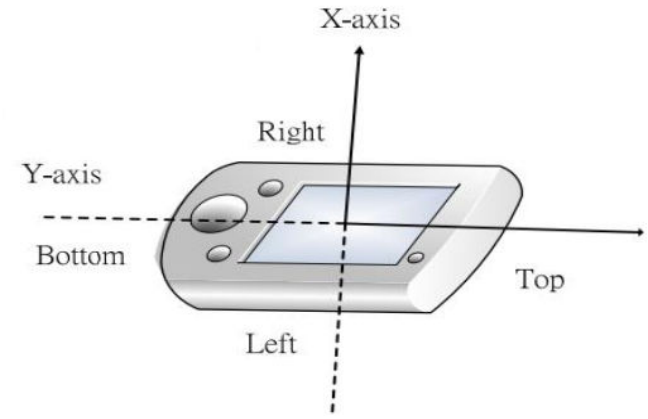

Figure 6: Triaxial Direction of the Mobile Phone Place in the Vehicle (Bai *et al.*, 2012)

Table 1: Significance of Triaxial Directions

Measurements Obtained

Axis	**Direction**	**Typical Driving**
X	Up/Down	Vibration/Road Undulations
Y	Front/Rear	Acceleration/Braking
Z	Left/Right	Turning/Lane Changes

C. Validation of Experimental Data Using Xcos Block Model

The mathematical model obtained for the equation of motion (Equation 4-7) of a half semi-truck suspension system was represented with a `time-based block diagram' shown in Figure 7 to simulate a hybrid dynamic system, including continuous and discrete models. The integration block from the Xcos module in SCILAB software was utilised to integrate a higher derivative value to a lower one, i.e. from acceleration to velocity to displacement, and the acceleration of the sprung mass and unsprung mass was integrated to obtain the velocity and also integrated to obtain the displacement of the system. The experimental results were utilised as input for the half semi-truck suspension system simulation.

III. RESULTS AND DISCUSSION

The experimental data collected from 0 to 5 seconds using a smartphone for the half semi-truck vehicle are presented in Table 2 at 10 to 30 km/h speed. The data shows the records of the vehicle vibration on road irregularities and bumps in both the x and y directions. It can be observed that at time zero, the vibration of the vehicle before motion has the acceleration Ax (0.2928 m/s^2), Ay (-0.09864 m/s^2) at 10 km/h, Ax (0.6513 m/s^2), Ay (1.2295 m/s^2) at 20 km/h and Ax (0.6478 m/s^2), Ay (-0.7667 m/s^2) at 30 km/h. These can be attributed to the accelerometer's sensitivity to small movements during setup.

As the vehicle crosses the bump, the accelerations are higher and lower on the smooth road. The acceleration values were obtained as processing the data to study the behaviour of ride comfort. The relatively stable baseline acceleration level near zero was observed on the graph. This baseline represents the device's inherent sensor and the influence of gravity when there is no motion.

Acceleration peaks during vibration at 10 km/h speed as shown in Figure 8. It revealed the periodic peaks, troughs, and fluctuations in acceleration indicate the suspension system responds to the simulated road conditions. The positive peak corresponds to the upward vertical excitation experienced by the suspension system, typically due to encountering bumps or road irregularities. The negative peaks correspond to downward acceleration as it returns to its resting position after crossing road undulation (bumps). In this case, with a speed of 10, 20 and 30 km/h as shown in Figures 8 to 10, the maximum Root mean square (RMS) acceleration was obtained at 0.31, 0.54, and 0.69 m/s^2 for 0.08 bumps height, respectively. It is observed that RMS acceleration values of the speed 10 km/h are below 0.315 m/s^2, which indicates the passenger or users are not in uncomfortable zones.

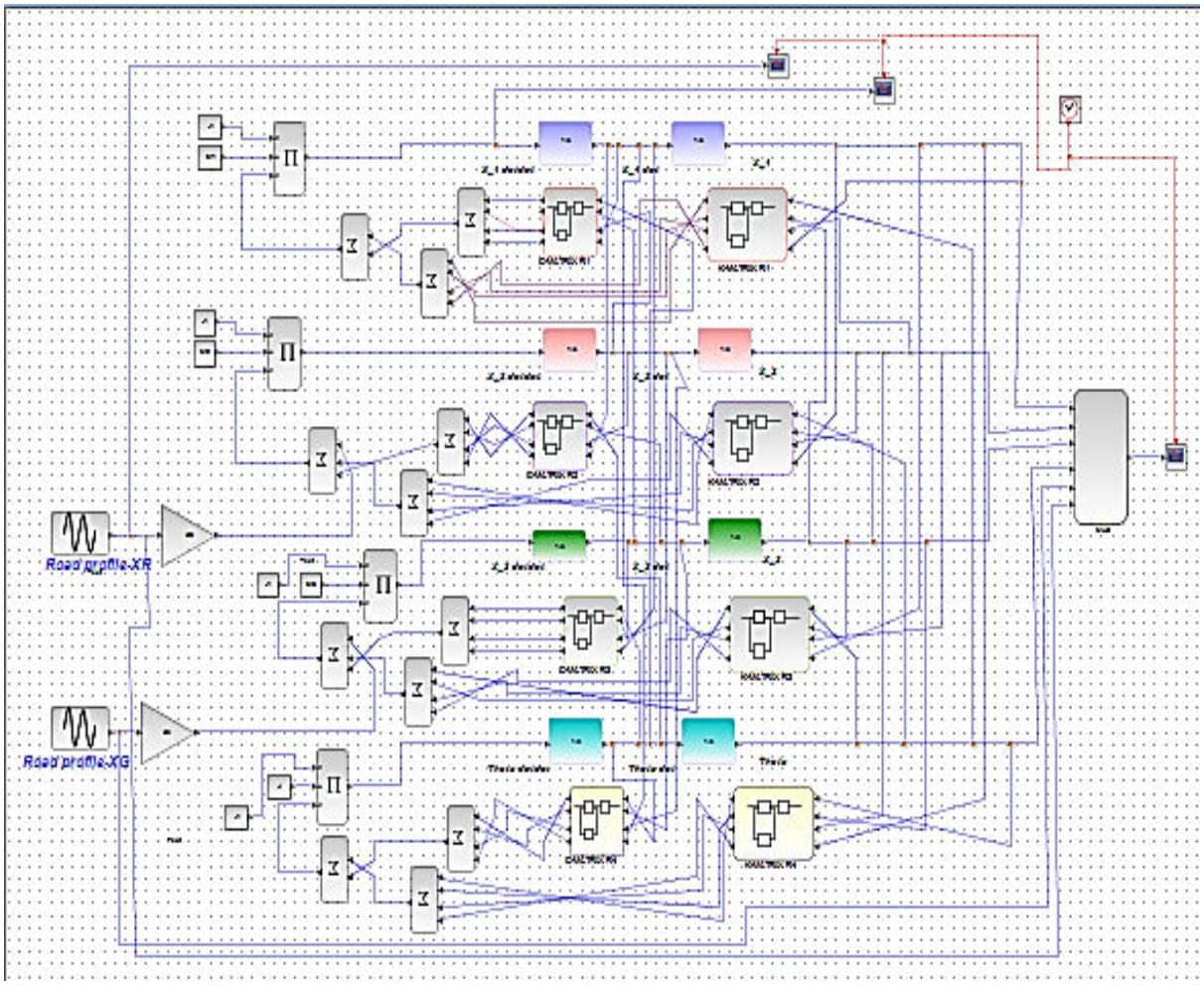

Figure 7: SCILAB-Xcos Model for Half-Car

Table 2: Acceleration and Time at 10 km/h with Brake

	10 km/h		20 km/h		30 km/h	
Time (sec)	**Ax (m/s²)**	**Ay (m/s²)**	**Ax (m/s²)**	**Ay (m/s²)**	**Ax (m/s²)**	**Ay (m/s²)**
0	0.2928	-0.09864	0.651305	1.229513	-0.2658	-0.76666
0.52	0.240329	0.093341	0.613305	1.152513	0.232199	0.076341
1.02	0.5098	0.228581	0.690305	-0.03448	-0.3048	0.728341
1.51	-0.8978	0.503341	0.001305	1.382513	0.6478	0.498341
2.02	0.6758	0.689341	0.345305	-1.10748	-0.2658	0.689341
2.52	0.4358	0.421341	0.460305	-2.37048	0.4958	0.421341
3.02	-0.2308	0.383341	-1.68369	-0.95445	-0.3808	0.383341
3.52	-0.18	0.229341	0.70669	-0.34143	0.1508	0.229341
4.01	-0.1308	0.056341	-0.99469	-0.95442	-0.1128	0.038341
4.52	1.976595	3.348341	2.75831	-1.37548	1.113199	2.260341
5.02	-0.6528	0.343451	1.22631	0.99951	-0.2278	0.229341

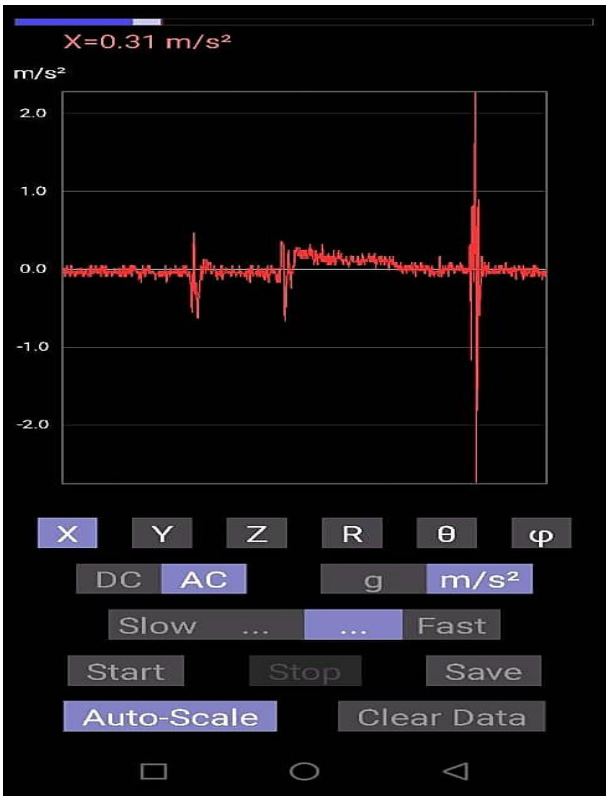

Figure 8: Variation of Acceleration against Time for the Vibration of Semi-truck at 10 km/h Speed

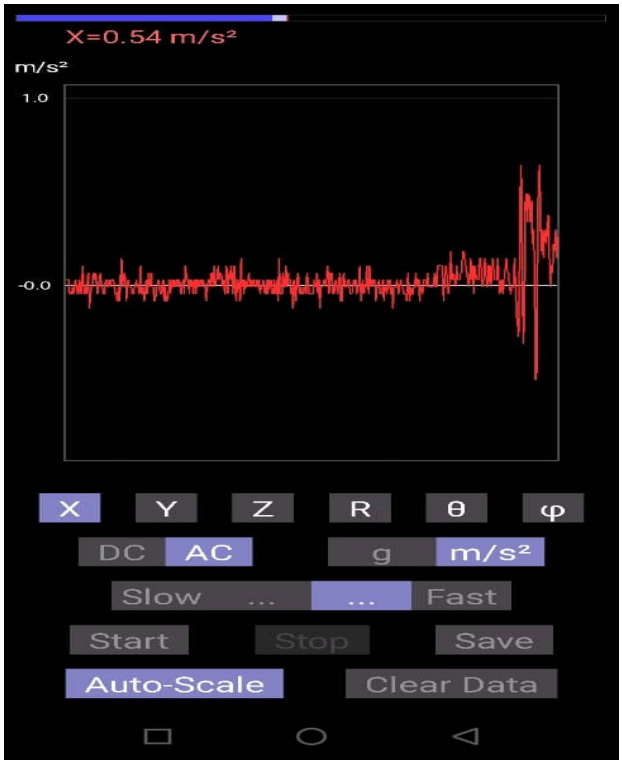

Figure 9: Variation of Acceleration against Time for the Vibration of Semi-truck at 20 km/h Speed

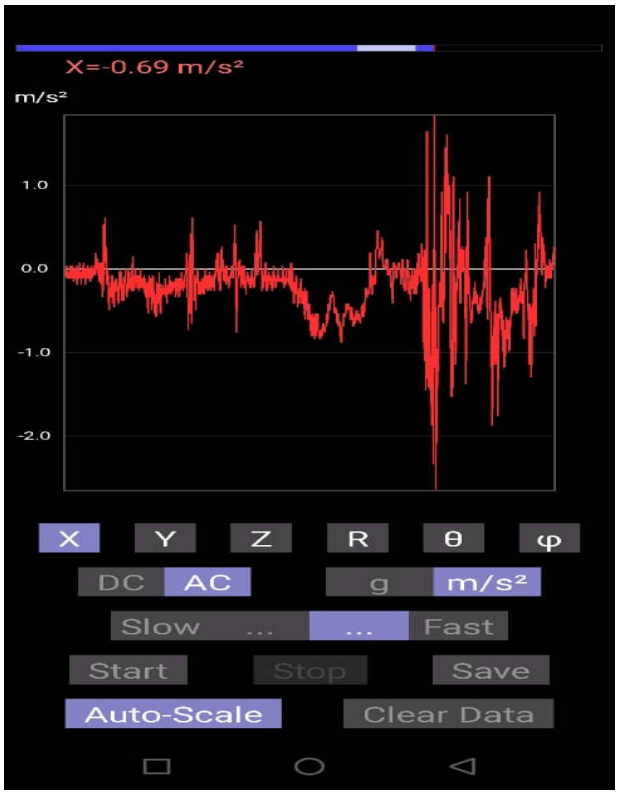

Figure 10: Variation of Acceleration against Time for the Vibration of Semi-truck at 30 km/h Speed

According to ISO 2631-1-1997, it has been established that when RMS acceleration is less than 0.315 m/s^2, the passenger is not in an uncomfortable zone (Medina *et al.,* 2023). However, Han and Zhang (Guoxi and Shuguang, 2011) reported that ranges of 0.315 to 0.63 m/s^2, 0. 5 to 1 m/s^2, 0.8 to 1.6 m/s^2, 1.25 to 2.5 m/s^2 and Great than 2 m/s^2 are considered to be a little uncomfortable, fairly uncomfortable, uncomfortable, very uncomfortable and extremely uncomfortable, respectively. As a result, the vehicle at the 20 and 30 km/h speeds exhibited slightly higher RMS acceleration, indicating a little discomfort experienced by the passenger.

A. Simulations

The numerical and computational models were implemented to fully understand the requirements for system identification of the vehicle parameters. The modelling includes road profile generation and vehicle simulation. Input needs were provided to the vehicle to excite a response from the system to perform parameter identification. A speed bump obtains an acceleration response with a strong signal-to-noise ratio. The vehicle parameters used in the simulation are shown in Table 3. Typical speed bump was modelled as a cosine function with the displacement of the vehicle body at bump height of 0.08 meters, shown in Figures 11 to 13.

Table 3: The Required Parameters for the simulation

Sprung Mass (M_1)	**1238 kg**
Front Suspension Stiffness (K2)	40,000 N/m
Rear Suspension Stiffness (K1)	30,000 N/m
Front Damping Coefficient (C2)	5000 N.s/m
Rear Damping Coefficient (C1)	5000 N.s/m
Front Unsprung Mass (M3)	120 kg
Rear Unsprung Mass (M2)	120 kg
Front Tire Stiffness (K4)	250,000 N/m
Rear Tire Stiffness (K3)	250,000 N/m
L_1	1.8 m
L_2	1.2 m
Moment of Inertial (J)	1000 Ns^2/kg

The y-axis represents the displacement of the vehicle body, while the x-axis denotes the corresponding time or distance. As the vehicle approaches the speed bump, the displacement remains relatively constant, indicating that its body is in its normal position. However, as the vehicle encounters the speed bump, the displacement abruptly increases, signifying the upward movement of the vehicle body due to the impact. The graph's peak represents the maximum displacement achieved during this upward motion. Following the peak, the displacement decreases as the vehicle descends from the speed bump, eventually returning to its normal position.

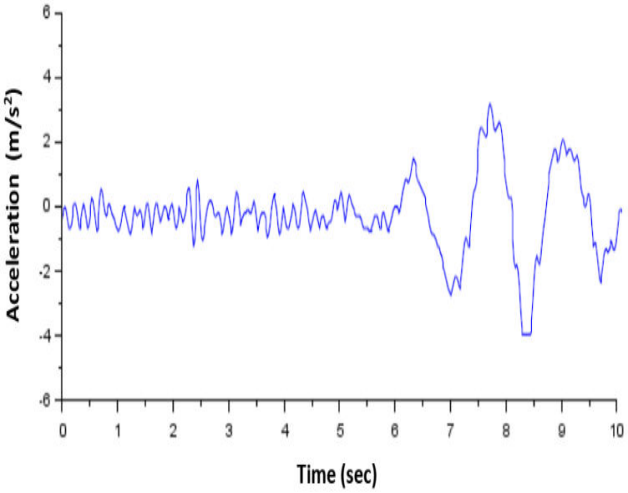

Figure 11: Simulated Acceleration against Time over 0.08 m Bump at 10 km/h Speed

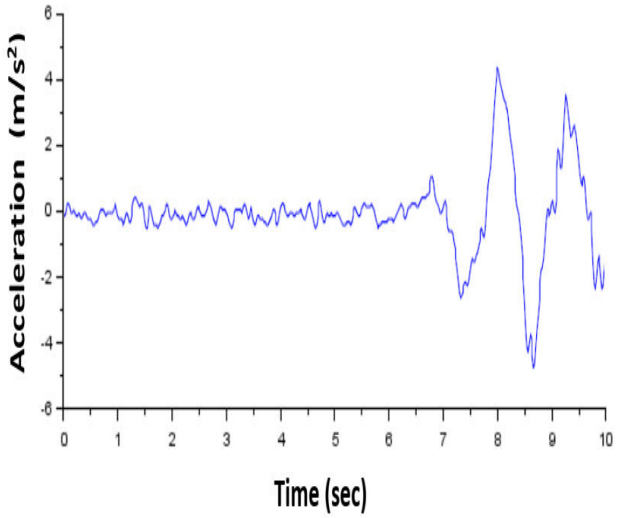

Figure 12: Simulated Acceleration Against Time over 0.08 m Bump at 20km/h Speed

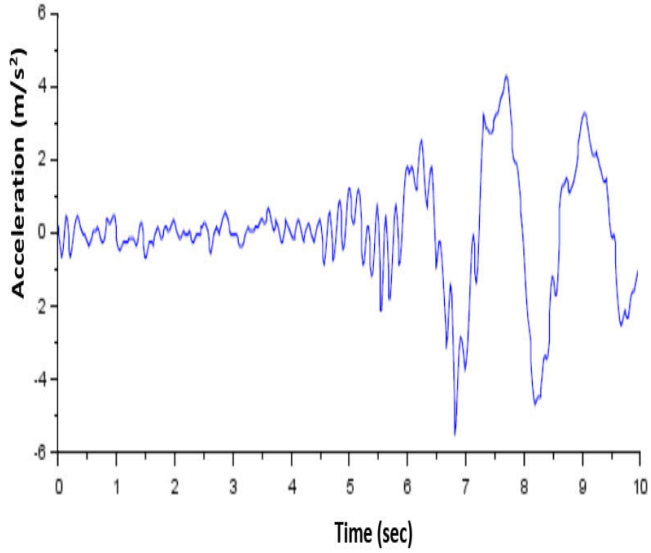

Figure 13: Simulated Acceleration Against Time over 0.08 m Bump at 30km/h Speed

Figures 11 to 13 showed the variation of acceleration against time for the vibration of a semi-truck suspension model with the speeds (10, 20, and 30 km/h) and bump height of 0.08 meters. The acceleration peaks and troughs are closer at higher speeds, indicating a shorter vibration duration. This is because the truck is covering more ground in less time. The amplitude (height) of the peaks and troughs also increases with higher speeds, reflecting the more significant force exerted on the suspension system when encountering bumps at higher velocities. Consequently, a higher acceleration is needed with a bump height, as the suspension system needs to provide more force to overcome the greater obstacle.

The simulated maximum RMS acceleration for the half truck model at 10, 20 and 30 km/h speeds were obtained as 0.325, 0.546 and 0.722 m/s^{2,} respectively. The RMS accelerations agreed with the results obtained from the mobile accelerometer with percentage errors of 4.6%, 1.1% and 4.18%, respectively which is consistent with the Wang *et al.* (2022) findings. However, the RMS value obtained at a 10 km/h speed, is slightly higher than the RMS values obtained from the mobile accelerometer. This could be because of the insensitivity of the accelerometer to the low speed of less than equal to 10 km/h. However, it can be observed from the simulated results that the RMS accelerations at 10, 20 and 30 km/h speed are considered fairly uncomfortable for the passenger. Wawryszczuk *et al.* (2023) reported that a fairly uncomfortable zone is achieved for ride comfort with the vehicle moving at 10 to 100 km/h speed range. And proven that road handling is very high at low speeds and maximum at 20 km/h, then decreases drastically, but after 45 km/h, increasing velocity does not have any effect on the bump of height 0-0.1m. The simulation results are consistence with Nguye's (2023) findings on the vibration analysis of an active suspension system using PID-SMC synthetic control algorithm to ensure road holding and ride comfort. As the vehicle speed increases, the impact of the bump or road irregularity on the vehicle's body becomes more pronounced. At higher speeds (30 km/h), the vehicle's suspension system did not have enough time to absorb the bump's energy, leading to higher acceleration peak values. Therefore, the RMS acceleration generally increases as the speed increases. It has been established that Passengers' comfort depends on minimising the acceleration peaks, as excessive accelerations can lead to discomfort and potential vehicle damage (Goenaga *et al.,* 2020).

Figure 11 shows the acceleration against time for the vibration of a semi-truck suspension model provides a visual representation of how the system responds to different speeds at 0.08 bump height. It helps engineers and designers assess the performance of the suspension system and make necessary adjustments to improve ride comfort and safety.

Figure 14 shows the velocity of the vehicle against time at a speed of 10 to 30 km/h. The velocity increases with the increasing vehicle's speed and reaches the maximum at 0.08 m bump height, then reduces after the bump on the road and with a brake application. The maximum velocities are higher, with 3.82 m/s, 12.75 m/s and 56.35 m/s for the speeds of 10, 20 and 30 km/h, respectively. These results corroborate with higher maximum velocity (12.9 to 27.6 m/s) obtained for idle running car with forced 2,000 min/s, car not jacked up by Kazmierczak *et al.* (2010). The semi-truck velocity should ideally be always zero on the graph, regardless of the speed settings (10, 20, or 30 km/h).

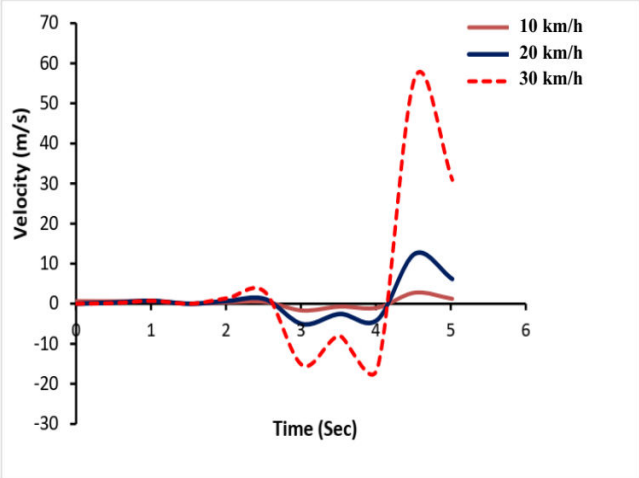

Figure 14: Variation of Velocity against Time for the Vehicle Vibration at 10 - 30 km/h Speed

IV. CONCLUSION

The use of a mobile app accelerometer for experimental data collection proved to be a practical and accessible method for capturing real-world suspension system responses. The model facilitated the prediction of system behaviour under controlled conditions and allowed for comparative analysis with experimental data. The variation in speed (10, 20, and 30 km/h) demonstrated that the suspension system's response is directly influenced by vehicle velocity. Higher speeds lead to more pronounced acceleration peaks and shorter vibration duration, reflecting the increased impact of road irregularities on the vehicle at elevated speeds. The bump heights resulted in higher amplitude acceleration peaks, indicating that the suspension system must exert greater force to overcome larger obstacles. The root mean square values provided a comprehensive measure of the overall level of vibration experienced by the vehicle and the users. The root mean square results complemented the acceleration and displacement data by offering a single metric for assessing ride comfort and safety.

AUTHOR CONTRIBUTIONS

H. K. Ibrahim: Conceptualization, Methodology, Data curation; Validation, & editing; **O. T. Popoola:** Supervision, Resources; **E. A. Akinola:** Investigation, Funding acquisition, Writing – review & editing. **F. W. Osatuyi:** Investigation, Formal analysis; Writing – review. **Z. O. Tijani:** Formal analysis; Writing – review & editing; **K. O. Abdulazeez:** Formal analysis; Writing – review & editing; **F. O. Mustapha:** Investigation & Formal analysis; **T. M. Kelani:** Formal analysis; & Validation.

REFERENCES

Atindana, V. A., Xu, X., Nyedeb, A. N., Quaisie, J. K., Nkrumah, J. K., & Assam, S. P. (2023). The evolution of vehicle pneumatic vibration isolation: A systematic review. *Shock and Vibration*, *2023*(1), 1716615.

Bai, Y. W., Wu, S. C., & Tsai, C. L. (2012). Design and implementation of a fall monitor system by using a 3-axis accelerometer in a smart phone. *IEEE Transactions on Consumer Electronics*, *58*(4).

Bhagyasri, P., & Chaitanya M. M. (2019). Vibration and Suspension Deflection Controlling of Half Car Model using ANSYS and MATLAB. *International Research Journal of Engineering and Technology*.

Bovnegra, L., & Strelbitskyi, V. (2022). MODELING MASS-SPRING-DAMPER SYSTEM USING SCILAB. *Праці Одеського Політехнічного Університету*, *2*(66).

Casati, J. P. B., Altafim, R. A. C., & Altafim, R. A. P. (2020). Vibration Detection of Vehicle Impact Using Smartphone Accelerometer Data and Long-Short Term Memory Neural Network. In *Congresso Brasileiro de Automática-CBA*, *2*(1).

De La Torre, R. D., Pasobillo, G. A. E., Rebueno, M. F., Sunga, D. P., Esguerra, B. J. J., & Concepcion, R. (2020). Vibration-based Structural Health Monitoring System for Bridges using ADXL345 Accelerometer with MATLAB Standalone Application. *2020 IEEE 12th International Conference on Humanoid, Nanotechnology, Information Technology, Communication and Control, Environment, and Management, HNICEM 2020*.

Feldbusch, A., Sadegh-Azar, H., & Agne, P. (2017). Vibration analysis using mobile devices (smartphones or tablets). *Procedia Engineering*, *199*.

Ginart, A., Ali, I. N., Barlas, I. Ginart, A., Ali, I. N., Barlas, I., Ginart, A. A., Sheldon, J. S., Kalgren, P. W., & Roemer, M. J. (2011). Smart phone machinery vibration measurement. In *2011 Aerospace Conference* (pp. 1-7). IEEE

Goenaga, B., Underwood, S., & Fuentes, L. (2020). Effect of speed bumps on pavement condition. *Transportation Research Record*, *2674*(9).

Guoxi, H., & Shuguang, Z. (2011). Research on assessment indices of safety and comfort for flight in wind fields. *Procedia Engineering*, *17*.

Hapsari, A. A., Supriyanto, E., Hasan, A., & Suharjono, A. (2021). Accelerometer sensor data analysis of bridge structural health monitoring system. *IOP Conference Series: Materials Science and Engineering*, *1108*(1).

Ibrahim, A., Eltawil, A., Na, Y., & El-Tawil, S. (2020). Accuracy limits of embedded smart device accelerometer sensors. *IEEE Transactions on Instrumentation and Measurement*, *69*(8).

Jia, Z., & Sharma, A. (2021). Review on engine vibration fault analysis based on data mining. *Journal of Vibroengineering*, *23*(6).

Kazmierczak, A., Moczko, P., Kaźmierczak, A., Reksa, M., Moczko, P., & Wróbel, R. (2010). *Comparative Analysis of The Vibrations of a Spark-Ignition Engine with and without Supercharging, Mounted in New Motor Vehicles*.

Khemliche, M., Dif, I., Latreche, S., & Bouamama, B. O. (2004). Modelling and analysis of an active suspension 1/4 of vehicule with bond graph. *International Symposium on Control, Communications and Signal Processing, ISCCSP*.

Medina, A., Orozco Torres, J. A., Hernández Gracidas, C. A., Garduza, S. H., & Franco, J. D. (2023). Diagnosis and Study of Mechanical Vibrations in Cargo Vehicles Using ISO 2631-1:1997. *Sensors*, *23*(24).

Nguyen, T. A. (2021). Improving the Comfort of the Vehicle Based on Using the Active Suspension System Controlled by the Double-Integrated Controller. *Shock and Vibration*, *2021*.

Nguyen, T. A. (2023). Applying a PID-SMC synthetic control algorithm to the active suspension system to ensure road holding and ride comfort. *PLoS ONE*, *18*(10 October).

Ojolo, S. J., Ajayi, O. O., & Asuelinmen, G. A. (2021). Investigating the effect of vibration on the stability of the three-wheeled scooter taxi. *Nigerian Journal of Technology*, *39*(4).

Phalke, T. P., & Mitra, A. C. (2017). Analysis of Ride comfort and Road holding of Quarter car model by SIMULINK. *Materials Today: Proceedings*, *4*(2).

Piñón, A., Favela-Contreras, A., Félix-Herrán, L. C., Beltran-Carbajal, F., & Lozoya, C. (2021). An arx model-based predictive control of a semi-active vehicle suspension to improve passenger comfort and road-holding. *Actuators*, *10*(3).

Puneet, N. P., Hegale, A., Kumar, H., & Gangadharan, K. V. (2019). Multi objective optimization of quarter car parameters for better ride comfort and road holding. *AIP Conference Proceedings*, *2200*.

Rana, S., & Asaduzzaman. (2021). Vibration based pavement roughness monitoring system using vehicle dynamics and smartphone with estimated vehicle parameters. *Results in Engineering*, *12*.

Riley, C. (2023). Mobile Phone-Based Contact and Non-Contact Vibration Sensing for Structural Dynamics Teaching Laboratories. *ASEE Annual Conference and Exposition, Conference Proceedings*

Tiwari, A., & Bhavikatti, S. (2020). Study of Road Holding and Ride Comfort of Half Car Model using Mathematical Modelling. *IJSDR2011035 International Journal of Scientific Development and Research*.

Wang, X., Cheng, Z., & Ma, N. (2022). Road Recognition Based on Vehicle Vibration Signal and Comfortable Speed Strategy Formulation Using ISA Algorithm. *Sensors*, *22*(17).

Wawryszczuk, R., Kardas-Cinal, E., Lejk, J., & Sokołowski, M. (2023). Methods of Passenger Ride Comfort Evaluation—Tests for Metro Cars. *Sensors*, *23*(12).

Yaabari, N., Okoro, O. I., & Akpama, E. J. (2023). Matlab-based simulations of a three-phase induction motor for dynamic studies. *Nigerian Journal of Technology*, *41*(6).

Yatak, M. Ö., & Şahin, F. (2021). Ride Comfort-Road Holding Trade-off Improvement of Full Vehicle Active Suspension System by Interval Type-2 Fuzzy Control. *Engineering Science and Technology, an International Journal*, *24*(1), 259-270.